

Anisotropy of microwave conductivity of $\text{YBa}_2\text{Cu}_3\text{O}_{7-x}$ in superconducting and normal states: Crossover $3D - 2D$

M.R. Trunin, Yu.A. Nefyodov

Institute of Solid State Physics of RAS, 142432 Chernogolovka, Moscow region, Russia

Imaginary part of the microwave conductivity $\sigma''(T < T_c)$ and the resistivity $\rho(T) = 1/\sigma(T > T_c)$ along (σ''_{ab} and ρ_{ab}) and perpendicular to (σ''_c and ρ_c) cuprate ab -planes of $\text{YBa}_2\text{Cu}_3\text{O}_{7-x}$ crystal were measured in the temperature range $5 \leq T \leq 200$ K, having varied the oxygen doping level x in the crystal from 0.07 to 0.47. The superconducting state was found to have the dependences $\sigma''_{ab}(T)/\sigma''_{ab}(0)$ and $\sigma''_c(T)/\sigma''_c(0)$ coincide in the optimally doped ($x = 0.07$) crystal. With the increase of x the dependences $\sigma''_c(T)/\sigma''_c(0)$ have smaller slope at $T < T_c/3$ with $\sigma''_{ab}(T)/\sigma''_{ab}(0)$ changing slightly. The ab -plane transport in the normal state of $\text{YBa}_2\text{Cu}_3\text{O}_{7-x}$ crystal always remains metallic. However, a crossover from Drude conductivity (at $x = 0.07$) along the c -axis to the hopping one (at $x > 0.07$) takes place. This is proved by both estimating minimum metallic c -conductivity and maximum tunneling c -conductivity and quantitatively comparing the measured dependences $\rho_c(T)$ with the ones calculated in the polaron model of quasiparticles' c -transport.

Recently a lot of interest has been attracted by investigations of transport properties evolution in high-temperature superconductors (HTSC) with different level of doping by oxygen and other substitutional impurities; in other words, the dependence upon the number p of holes per Cu atom in the CuO_2 plane. The p value and the critical temperature T_c of a superconducting transition in HTSC satisfy the following empirical relationship¹: $T_c = T_{c,max}[1 - 82.6(p - 0.16)^2]$.

Up to now, the narrow band of HTSC phase diagram, corresponding to the optimal doping ($p \approx 0.16$) and maximum values of the critical temperature $T_c = T_{c,max}$, is the most studied area. In the normal state of optimally doped HTSC the resistivity $\rho_{ab}(T)$ of cuprate ab -planes increases proportionally to temperature, viz. $\Delta\rho_{ab}(T) \propto T$. The resistivity $\rho_c(T)$ in perpendicular direction substantially exceeds the value of $\rho_{ab}(T)$ and also has metallic behavior (both $\rho_{ab}(T)$ and $\rho_c(T)$ increase with T). Bi-2212, which is the most anisotropic HTSC (having $\rho_c/\rho_{ab} \approx 10^5$ at $p \approx 0.16$), represents an exception: its resistivity $\rho_c(T)$ increases as T approaches T_c ($d\rho_c(T)/dT < 0$). This Bi-2212 feature agrees with the estimate of the minimal metallic conductivity in the c -direction for anisotropic three-dimensional ($3D$) Fermi liquid model²:

$$\sigma_{c,min}^{3D} = \sqrt{\rho_{ab}/\rho_c} n e^2 d^2 / h, \quad (1)$$

where $n \approx 10^{21} \text{ cm}^{-3}$ is a $3D$ carrier concentration, d is lattice constant along the c -axis, h is Planck's constant. In Bi-2212 the conductivity $\sigma_c = 1/\rho_c \ll \sigma_{c,min}^{3D}$ at $T = T_c$, but the other optimally doped HTSC have $\sigma_c(T_c) > \sigma_{c,min}^{3D}(T_c)$. The conductivity $\sigma_{c,min}$ in (1) is less than Ioffe-Regel limit $\sigma_{IR} = e^2 k_F / h$ for the two-dimensional ($2D$) case, i.e., $\sigma_{c,min} \approx \sqrt{\rho_{ab}/\rho_c} \sigma_{IR} d/a \ll \sigma_{IR}$ ($a \approx 2\pi/k_F$ is the lattice constant in the CuO_2 plane), whereas $\sigma_{ab,min} \approx \sigma_{IR}^2$.

A measure of HTSC anisotropy in the superconducting state is the ratio $\sigma''_{ab}(0)/\sigma''_c(0) = \lambda_c^2(0)/\lambda_{ab}^2(0)$, where σ''_{ab} and σ''_c are imaginary parts of conductivity, λ_{ab} and λ_c are penetration depths of high-frequency field for

currents running in the ab -planes and perpendicular to them, correspondingly. It is common knowledge that $\Delta\lambda_{ab}(T) \propto T$ at $T < T_c/3$ in optimally doped high-quality HTSC and this experimental fact provides strong evidence for $d_{x^2-y^2}$ symmetry of the order parameter in these materials. However, there is no consensus in literature about $\Delta\lambda_c(T)$ behavior at low temperatures. Even $\text{YBa}_2\text{Cu}_3\text{O}_{6.95}$ ($T_c \approx 93$ K), the most thoroughly studied single crystals, have shown both linear, $\Delta\lambda_c(T) \propto T^{4,5,6}$, and quadratic dependences⁷ in the range $T < T_c/3$.

Pseudogap states, appearing at $p < 0.16$, occupy a wide band of HTSC phase diagram, which is far less investigated. Measurements of ac -susceptibility of oriented HTSC powders at $T < T_c$ show⁸ that their dependences $\sigma''_c(T)/\sigma''_c(0)$ have smaller slope at $T \rightarrow 0$ than $\sigma''_{ab}(T)/\sigma''_{ab}(0)$ do. The normal state of underdoped HTSC is characterized by non-metallic behavior of the resistivity $\rho_c(T)$ at T approaching T_c , by deviation of the resistivity from its linear dependence $\Delta\rho_{ab}(T) \propto T$ and by ρ_c/ρ_{ab} ratio rising dramatically with the decrease of p . A lot of theoretical models have been proposed to explain these properties, but there is none fully describing the evolution of the dependences $\sigma''_{ab}(T)$, $\sigma''_c(T)$ and $\rho_{ab}(T)$, $\rho_c(T)$ in the wide range of concentration p and temperature T . Moreover, the c -transport mechanism is not defined; in particular, it is not clear if it can be metallic (Drude), or at any p conductivity along the c -axis is determined by quasi-particles tunneling between cuprate layers, accompanied by their scattering both within the layers and between them.

The present paper analyzes the results of anisotropy measurements and evolution of temperature dependences of conductivity components in the $\text{YBa}_2\text{Cu}_3\text{O}_{7-x}$ crystal under varying oxygen doping in the range $0.07 \leq x \leq 0.47$. The crystal of a rectangular shape, with dimensions $1.6 \times 0.4 \times 0.1 \text{ mm}^3$, has been grown in a BaZrO_3 crucible. The measurements were made at the frequency of $\omega/2\pi = 9.4$ GHz and in the temperature range $5 \leq T \leq 200$ K. To change an oxygen content in the sample, we successively annealed the sample in the air at

Table I: Annealing temperatures and parameters characterizing doping and the anisotropy of the superconducting and normal state of $\text{YBa}_2\text{Cu}_3\text{O}_{7-x}$.

annealing temperature T , °C	critical temperature T_c , K	doping parameters		λ values at $T = 0$		$\Delta\lambda_c(T) \propto T^\alpha$ α	λ_c/λ_{ab} at $T = 0$	$\sqrt{\rho_c/\rho_{ab}}$ at $T = 200\text{K}$
		p	x	λ_{ab} , nm	λ_c , μm			
500	92	0.15	0.07	152	1.55	1.0	10	11
520	80	0.12	0.26	170	3.0	1.1	18	18
550	70	0.105	0.33	178	5.2	1.2	29	16
600	57	0.092	0.40	190	6.9	1.3	36	16
720	41	0.078	0.47	198	16.3	1.8	83	35

different $T \geq 500^\circ\text{C}$ specified in Table 1. Anisotropy was measured for each of the five crystal states. According to susceptibility measurements at the frequency of 100 kHz, superconducting transition width amounted to 0.1 K in the optimally doped state ($x = 0.07$), however, the width increased with the increase of x , having reached 4 K at $x = 0.47$. The temperatures of the superconducting transition were $T_c = 92, 80, 70, 57, 41$ K. The whole cycle of the microwave measurements included the following: (i) we measured the temperature dependences of the quality factor and of the frequency shift of the superconducting niobium resonator with the sample inside in the two crystal orientations with respect to the microwave magnetic field, transversal (T) and longitudinal (L); (ii) measurements in the T orientation gave the surface resistance $R_{ab}(T)$, reactance $X_{ab}(T)$ and conductivity $\sigma_{ab}(T)$ of the crystal cuprate planes in its normal and superconducting states; (iii) measurements in the L orientation gave $\sigma_c(T)$, $X_c(T)$, $R_c(T)$. See⁶ for the details of the measuring technique in the optimally doped $\text{YBa}_2\text{Cu}_3\text{O}_{6.95}$ crystal. We have also reported the temperature dependences of the surface impedance components of $\text{YBa}_2\text{Cu}_3\text{O}_{7-x}$ at various x in the short communication⁹.

Fig. 1 shows the dependences $\sigma''_{ab}(T)/\sigma''_{ab}(0)$ (open symbols) and $\sigma''_c(T)/\sigma''_c(0)$ (solid symbols) at $T \leq T_c$ for $\text{YBa}_2\text{Cu}_3\text{O}_{7-x}$ states with $T_c = 92$ K, $T_c = 70$ K and $T_c = 41$ K. Table 1 contains values of the penetration depths $\lambda_{ab}(0)$ and $\lambda_c(0)$ at $T = 0$. The temperature behavior of the dependences $\sigma''_{ab}(T)/\sigma''_{ab}(0)$ does not show dramatic change at varying p . The optimally doped state of $\text{YBa}_2\text{Cu}_3\text{O}_{6.93}$ features good matching of the temperature dependences $\sigma''_{ab}(T)/\sigma''_{ab}(0)$ and $\sigma''_c(T)/\sigma''_c(0)$. Only does the theory of the linear response of an anisotropic superconductor⁸ explain this observation. With decreasing p the temperature dependences $\sigma''_c(T)/\sigma''_c(0)$ at $T < T_c/3$ become substantially weaker than $\sigma''_{ab}(T)/\sigma''_{ab}(0)$.

The model¹⁰ is appropriate for comparison with the experimental data provided in the present paper. The model describes the following contributions to the c -transport of quasi-particles in the superconducting and normal HTSC states: (a) direct hopping between cuprate planes and (b) hopping accompanied by inelastic scattering on phonons, as well as elastic scattering on impurities lying between planes. The conductivity in the very

cuprate planes is considered to be a Drude one

$$\sigma_{ab} = \frac{e^2 \nu_{2D} D_{ab}}{d} = \frac{n_{2D} e^2 \tau}{md}, \quad (2)$$

where $\nu_{2D} = m/\pi\hbar^2$ is the $2D$ density of states, $D_{ab} = v_F^2 \tau / 2$, v_F , τ and $n_{2D} = k_F^2 / 2\pi$ are the diffusion coefficient, Fermi velocity, relaxation time and the $2D$ density of quasi-particles in the ab -plane, correspondingly. The total Hamiltonian of the electronic system in the model¹⁰ represents a sum of Hamiltonians of m individual CuO_2 layers, $\sum_m H_m$, and an inter-layer coupling Hamiltonian H_\perp , which is considered small in comparison with $\sum_m H_m$. This resulted in the perturbation theory calculations to the second order of H_\perp showing that the quasi-particles transport between neighboring weakly-coupled layers is analogous to tunneling in the SIS junction at

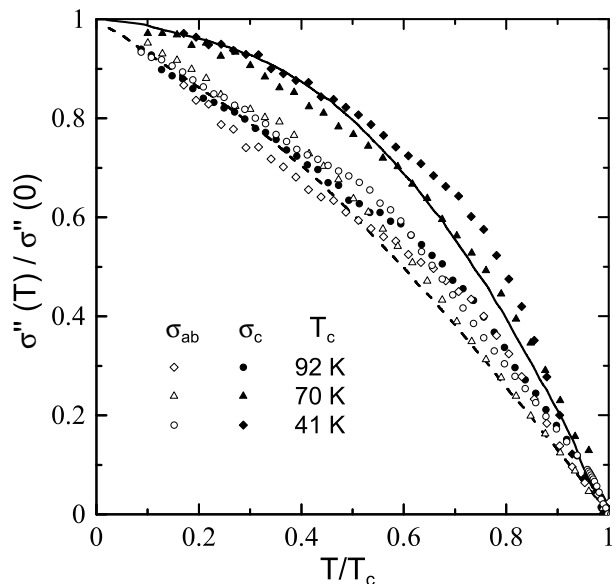


Figure 1: The dependences $\sigma''_{ab}(T)/\sigma''_{ab}(0)$ (open symbols) and $\sigma''_c(T)/\sigma''_c(0)$ (full symbols) measured for the three states of the $\text{YBa}_2\text{Cu}_3\text{O}_{7-x}$ crystal with $T_c = 92$ K, $T_c = 70$ K and $T_c = 41$ K. Solid and dashed lines stand for the dependences $\sigma''_c(T)/\sigma''_c(0)$ and $\sigma''_{ab}(T)/\sigma''_{ab}(0)$ calculated in¹⁰ for $\text{YBa}_2\text{Cu}_3\text{O}_{7-x}$ with oxygen deficit.

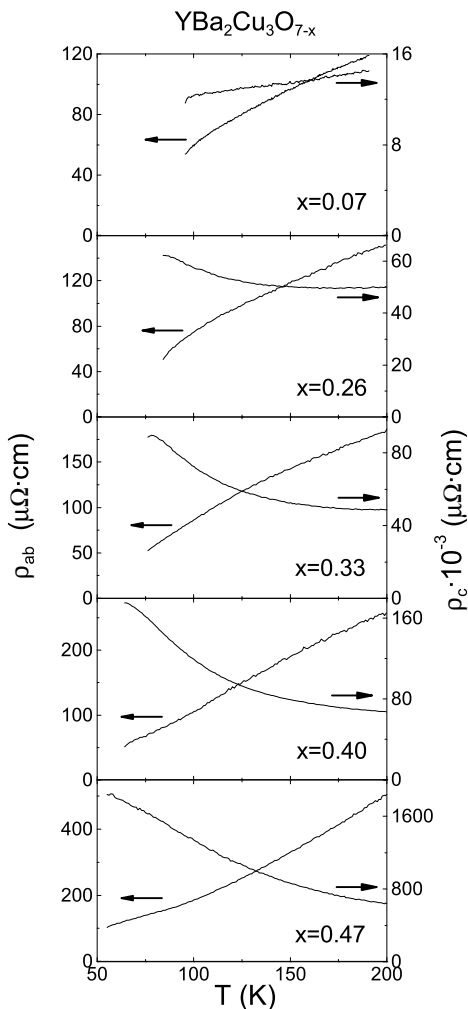


Figure 2: The evolution of the measured $\rho_{ab}(T)$ and $\rho_c(T)$ dependences in $\text{YBa}_2\text{Cu}_3\text{O}_{7-x}$ with different oxygen content.

$T < T_c$ and in the NIN junction at $T > T_c$. In addition, in the process (a) the electron ab -plane momentum is conserved (specular tunneling), whereas in the process (b) is not (diffusive tunneling)¹¹.

The authors of¹⁰ used the BCS model with d -symmetry of the order parameter in CuO_2 layers to calculate anisotropy of the superconducting HTSC state. Fig. 1 represents numerical results, calculated taking into account both of the processes (a) and (b), for $\sigma_c''(T)/\sigma_c''(0)$ (solid line) and for $\sigma_{ab}''(T)/\sigma_{ab}''(0)$ (dashed line). Having compared this with the experimental data at $T < T_c/2$ for $\text{YBa}_2\text{Cu}_3\text{O}_{7-x}$, with oxygen deficiency $x > 0.07$, one can see dramatic decrease in the slopes of the dependences $\sigma_c''(T)/\sigma_c''(0)$ with the increase of x , as well as insignificant change of the dependences $\sigma_{ab}''(T)/\sigma_{ab}''(0)$. The larger slopes of the experimental dependences in comparison with the theoretical ones at $T > T_c/2$ may be due to the effects of a strong electron-phonon interaction³, which are not taken into account in the model¹⁰. The dashed line in the Fig. 1 also coincides with the dependence $\sigma_c''(T)/\sigma_c''(0)$, calculated in¹⁰ in the ab-

sence of diffusive tunneling (b), when the specular tunneling process (a) along the c -axis becomes identical to the c -transport in the $3D$ superconductor. This exceptional case corresponds to the optimally doped $\text{YBa}_2\text{Cu}_3\text{O}_{6.93}$.

The real and imaginary parts of the surface impedance of the $\text{YBa}_2\text{Cu}_3\text{O}_{7-x}$ crystal, measured for each value of x in the Table 1, were found to coincide at $T > T_c$ ⁹: $R_{ab}(T) = X_{ab}(T)$, $R_c(T) = X_c(T)$. Therefore, the resistivities $\rho_{ab}(T)$ and $\rho_c(T)$ were found from $R_{ab}(T)$ and $R_c(T)$, applying the usual formulas of the normal skin effect: $\rho_{ab}(T) = 2R_{ab}^2(T)/\omega\mu_0$, $\rho_c(T) = 2R_c^2(T)/\omega\mu_0$. Fig. 2 shows the evolution of the dependences $\rho_{ab}(T)$ and $\rho_c(T)$ in the range $T_c < T \leq 200$ K with the change of x . The last column in Table 1 contains $(\rho_c/\rho_{ab})^{1/2}$ values at $T = 200$ K. Only the optimally doped $\text{YBa}_2\text{Cu}_3\text{O}_{6.93}$ shows that both dependences $\rho_{ab}(T)$ and $\rho_c(T)$ have a metallic behavior, and the ratio ρ_c/ρ_{ab} approaches the anisotropy of effective masses of charge carriers $m_c/m_{ab} = \lambda_c^2(0)/\lambda_{ab}^2(0)$ in the pure $3D$ London superconductor, which type $\text{YBa}_2\text{Cu}_3\text{O}_{6.93}$ belongs to. The other states of $\text{YBa}_2\text{Cu}_3\text{O}_{7-x}$ with lower concentration of holes have the resistivity $\rho_c(T)$ increase with the decrease of temperature, which shows its non-metallic behavior. Fig. 3 represents the experimental dependences $\sigma_c(T)$ compared to the values of $\sigma_{c,min}^{3D}$, calculated using the formula (1) for the three states of the $\text{YBa}_2\text{Cu}_3\text{O}_{7-x}$ crystal with $T_c = 92$ K (dashed line), $T_c = 70$ K (dotted line) and $T_c = 41$ K (dash-dotted line). It is only the c -axis conductivity of $\text{YBa}_2\text{Cu}_3\text{O}_{6.93}$ that exceeds the minimum metallic value of $\sigma_{c,min}^{3D}$ in the whole temperature range.

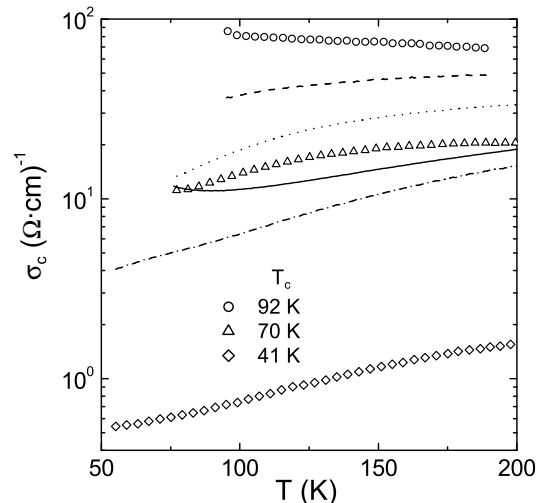


Figure 3: The symbols show for the experimental $\sigma_c(T)$ dependences in three states of $\text{YBa}_2\text{Cu}_3\text{O}_{7-x}$ at $T_c = 92$ K, $T_c = 70$ K and $T_c = 41$ K. The dashed, dotted and dash-dotted lines stand for the values of $\sigma_{c,min}^{3D}(T)$, corresponding to these states and obtained from the formula (1) using the measured $\rho_{ab}(T)$ and $\rho_c(T)$ in Fig. 2. The solid line represents calculations of $\sigma_c(T)$ using the formulas from¹⁰ for $\text{YBa}_2\text{Cu}_3\text{O}_{6.67}$.

Thus, it is natural to assume that as well as in the superconducting state of $\text{YBa}_2\text{Cu}_3\text{O}_{7-x}$, a slight decrease in the carriers concentration (in comparison with the optimal level) in the normal state results in the crossover from 3D metallic conductivity to 2D Drude conductivity in CuO_2 layers and tunneling conductivity between these layers (the crossover 3D-2D). To analyze this assumption, the model¹⁰ again proves to be appropriate. If t_\perp is the interplane hopping matrix element, the c -conductivity of quasi-particles in the process (a) will be as follows^{10,11,12,13}:

$$\sigma_c^{dir} = 2e^2\tau\nu_{2D} \left(\frac{t_\perp}{\hbar}\right)^2 = 4\sigma_{ab} \left(\frac{t_\perp d}{\hbar\nu_F}\right)^2, \quad (3)$$

where $2\tau(t_\perp/\hbar)^2$ is the intensity of the direct tunneling between neighboring CuO_2 layers, σ_{ab} is the conductivity (2) in these layers. For this case the typical hopping time \hbar/t_\perp significantly exceeds the relaxation time τ in the plane¹¹: $\hbar/t_\perp \gg \tau$. The opposite limit $\hbar/t_\perp \ll \tau$ corresponds to Drude conductivity in all three directions, as in an anisotropic 3D metal. When $\hbar/t_\perp \approx \tau$, a crossover takes place. The maximal value of tunneling c -conductivity $\sigma_{c,max}^{dir} = 2\sigma_{IR}\sqrt{\rho_{ab}/\rho_c}$ from (3) is then reached, which is approximately equal to the minimal metallic conductivity $\sigma_{c,min}^{3D}$ from (1). In the case of diffusive tunneling of quasi-particles (processes (b) in the model¹⁰), conductivity along the c -axis equals^{11,14}

$$\sigma_c^{diff} = \frac{e^2\nu_{2D}D_c}{d} = \frac{e^2\nu_{2D}d}{\tau_c}, \quad (4)$$

where $D_c = d^2\tau_c$ is the diffusion coefficient and $1/\tau_c$ is the probability of scattering between cuprate planes. As in the previous case, at $\tau_c \approx \tau$ we find $\sigma_{c,max}^{diff} = \sigma_{IR}\sqrt{\rho_{ab}/\rho_c} \approx \sigma_{c,min}^{3D}$, and from (2) and (4) we obtain another representation of the 3D-2D transition criterion:

$$\sigma_{c,max}\sigma_{ab} \approx \frac{n_{2D}}{\pi} \left(\frac{e^2}{\hbar}\right)^2. \quad (5)$$

At $n_{2D} = n/d \approx 10^{14} \text{ cm}^{-2}$ the formula (5) demonstrates that the crossover 3D-2D appears when the value of $\rho_c\rho_{ab} \approx 10^{-6} (\Omega\cdot\text{cm})^2$ is reached. The data in the Fig. 2 gives $\rho_c\rho_{ab} \lesssim 10^{-6} (\Omega\cdot\text{cm})^2$ at $x = 0.07$ only, which confirms that the 3D anisotropic Fermi-liquid model is applicable to explaining the properties of the optimally doped $\text{YBa}_2\text{Cu}_3\text{O}_{6.93}$.

Two temperature dependences, with distinction of kind, of the c -conductivities at $T \geq T_c$ are followed from the formulas (3) and (4): for the case of the direct tunneling, $\sigma_c^{dir}(T) \propto \sigma_{ab}(T)$ rises with the increase of $\tau(T)$ at T approaching T_c , while $\sigma_c^{diff}(T)$ falls with the increase of $\tau_c(T)$. According to the model¹⁰, the total conductivity σ_c along the c -axis equals the sum of the conductivities, which are in turn determined by each of the above processes, (a) and (b). In the vicinity of T_c , it is scattering of quasi-particles on impurities, lying between cuprate planes, that determines σ_c^{diff} , which is not

temperature dependent, as long as another contribution to σ_c^{diff} , arising due to interaction with phonons, vanishes with temperature decrease. Vice versa, at $T \gg T_c$ the phonon contribution becomes prevailing. Thus, we have the following approximate temperature dependence for the conductivity $\sigma_c(T)$: $A/T + C + BT$ (A, B, C are temperature independent), which does not allow for our experimental data (the solid line in Fig. 3 represents an example of calculating $\sigma_c(T)$ using formulas from¹⁰ for the sample $\text{YBa}_2\text{Cu}_3\text{O}_{6.67}$).

However, very recently another c -transport model was proposed¹⁵, well describing all the dependences $\rho_c(T)$ shown in Fig. 2. Unlike¹⁰, where the effects of interaction with phonons appear in the second order of the perturbation theory, in the model¹⁵ the Hamiltonian allows for these effects accurately through a canonical transformation¹⁶; it is only after this interplanar tunneling of quasi-particles is considered as a perturbation of an electron-phonon system, which was strongly coupled initially. Such consideration is applicable if $\epsilon_F \gg \omega_0 \gg t_\perp$, where ϵ_F is Fermi energy, ω_0 is a typical phonon energy. Both inequalities hold for layered anisotropic HTSC, where according to¹⁵ in the c -direction an electron is surrounded by a large number of phonons, forming a polaron¹⁷ which influences the transversal ab -transport weakly. The following analytic expression was obtained in¹⁵ for Einsteinian spectrum of c -polarized phonons in the temperature range $T \sim \omega_0$:

$$\rho_c(T) \propto \rho_{ab}(T) \frac{\exp[g^2 \tanh(\omega_0/4T)]}{\sqrt{\sinh(\omega_0/2T)}}, \quad (6)$$

where g is a parameter characterizing strength of electron-phonon interaction, $g > 1$. Fig. 4 represents our result of comparing experimental dependences $\rho_c(T)$ (symbols) and those calculated from (6) (solid lines).

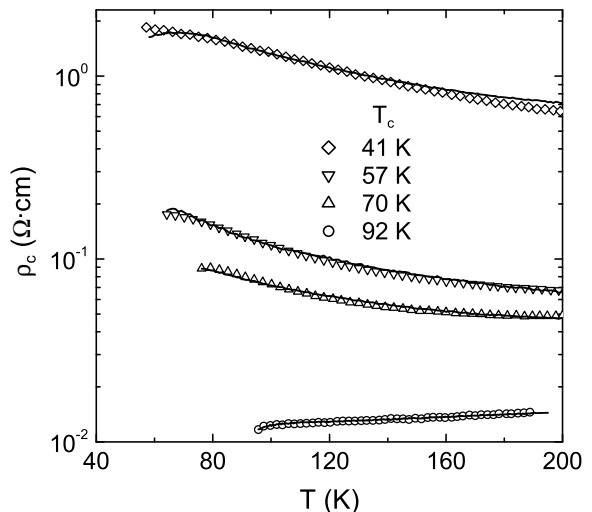


Figure 4: Comparison of the experimental dependences $\rho_c(T)$ in $\text{YBa}_2\text{Cu}_3\text{O}_{7-x}$ (symbols) and those calculated from (6) (solid lines).

To calculate them, we used $\rho_{ab}(T)$ data in Fig. 2; g was almost the same for all the dependences in Fig. 4: $g \approx 3$; ω_0 increased from 110 K (75 cm^{-1}) to 310 K (215 cm^{-1}) when the oxygen content ($7-x$) was decreased in $\text{YBa}_2\text{Cu}_3\text{O}_{7-x}$ from 6.93 to 6.53. In this connection, it seems quite natural to observe the anomalies of optical c -conductivity of $\text{YBa}_2\text{Cu}_3\text{O}_{7-x}$ crystals with oxygen deficiency in this frequency range¹⁸.

Thus, this paper represents the measurements of anisotropy of microwave conductivity of $\text{YBa}_2\text{Cu}_3\text{O}_{7-x}$ crystal, having varied the holes concentration p in the range $0.08 \leq p \leq 0.15$. Having analyzed temperature dependences of imaginary parts of the conductivity tensor

$\hat{\sigma}''(T)$ in the superconducting state and the resistivity $\hat{\rho}(T)$ in the normal state, we have demonstrated that the optimally doped $\text{YBa}_2\text{Cu}_3\text{O}_{6.93}$ is a tree-dimensional anisotropic metal. Decrease of carriers concentration in it results in the crossover from Drude c -axis conductivity to the hopping one. Moreover, to quantitatively describe the evolution of the dependences $\sigma_c''(T)$ and $\rho_c(T)$ at varying p , it is necessary to allow for the effects of strong electron-phonon interaction.

The authors acknowledge V.F. Gantmakher and A.F. Shevchun for valuable discussions. This work was supported by RFBR Grants Nos. 03-02-16812, 03-02-06386, 02-02-08004.

-
- ¹ J.L. Tallon, C. Bernhard, H. Shaked et al., Phys. Rev. B **51**, 12911 (1995).
² Y.B. Xie, Phys. Rev. B **45**, 11375 (1992).
³ M.R. Trunin and A.A. Golubov, in *Spectroscopy of High- T_c Superconductors. A Theoretical View* (Taylor and Francis, London and New York, 2003), pp.159-233.
⁴ J. Mao, D.H. Wu, J.L. Peng et al., Phys. Rev. B **51**, 3316 (1995).
⁵ H. Srikanth, Z. Zhai, S. Sridhar et al., J. Phys. Chem. Solids **59**, 2105 (1998).
⁶ Yu.A. Nefyodov, M.R. Trunin, A.A. Zhohov et al., Phys. Rev. B **67**, 144504 (2003).
⁷ A. Hosseini, S. Kamal, D.A. Bonn et al., Phys. Rev. Lett. **81**, 1298 (1998).
⁸ T. Xiang, C. Panagapoulos, and J.R. Cooper, Int. Journ. Mod. Phys. B **12**, 1007 (1998).
⁹ Yu.A. Nefyodov and M.R. Trunin, Physica C **388-389**, 469 (2003).
¹⁰ R.J. Radtke, V.N. Kostur, and K. Levin, Phys. Rev. B **53**, R522 (1995); R.J. Radtke and K. Levin, Physica C **250**, 282 (1995); R.J. Rojo and K. Levin, Phys. Rev. B **48**, 16861 (1993).
¹¹ M. Turlakov and A.J. Legget, Phys. Rev. B **63**, 064518 (2001).
¹² N. Kumar and A.M. Jayannavar, Phys. Rev. B **45**, 5001 (1992).
¹³ L.B. Ioffe, A.I. Larkin, A.A. Varlamov et. al., Phys. Rev. B **47**, 8936 (1993).
¹⁴ M.J. Graf, D. Rainer, and J.A. Sauls, Phys. Rev. B **47**, 12089 (1993).
¹⁵ A.F. Ho and A.J. Schofield, cond-mat/0211675.
¹⁶ I.G. Lang and Yu.A. Firsov, Sov. Phys. JETP **16**, 1301 (1963).
¹⁷ T. Holstein, Ann. of Phys. **8**, 343 (1959).
¹⁸ T. Timusk and B. Statt, Rep. Prog. Phys. **62**, 61 (1999).